# Electric transport in Fe/ZnSe/Fe heterostructures

H. C. Herper, P. Weinberger, and A. Vernes
*Center for Computational Materials Science, Gumpendorferstrasse 1a, A-1060 Vienna, Austria*

L. Szunyogh
*Department of Theoretical Physics, Budapest University of Technology and Economics, Budafoki út 8, H-1521, Budapest, Hungary and Center for Computational Materials Science, Gumpendorfer Strasse 1a, A-1060 Vienna, Austria*

C. Sommers
*Laboratoire de Physique des Solides, Université de Paris-Sud, 91405 Orsay, France*
(Received 22 May 2001; published 25 October 2001)

The electronic structure, magnetic properties, and perpendicular electric transport in bcc Fe/ZnSe/Fe(100) heterostructures with Zn and Se termination are discussed in terms of the fully relativistic spin-polarized version of the screened Korringa-Kohn-Rostoker method and the Kubo-Greenwood equation. It is found that different (Zn or Se) terminations cause substantial differences in the interlayer exchange coupling, the magnetic anisotropy, and, most prominently, in the magnetoresistance. The most important result, however, is that the difference between the sheet resistances in the parallel and the antiparallel configuration becomes constant with increasing spacer thickness. This constant value depends on the type of termination and is essentially determined by the interfaces.

DOI: 10.1103/PhysRevB.64.184442 PACS number(s): 75.30.Gw, 75.70.Ak, 75.70.Cn

## I. INTRODUCTION

Both, the growth of Fe(001) films on ZnSe(001) (Refs. 1–3) as well as of ZnSe epilayers on Fe(001) films[4] has been studied in the past using a variety of experimental tools. These studies were primarily performed in the search for systems that eventually would show a substantial magnetoresistance and therefore might turn out to be of technological interest. In the case of Fe/ZnSe systems it was argued that ZnSe is a direct wide band gap semiconductor[5] and that the lattice mismatch of 1.1% between ZnSe and twice the lattice constant of Fe is comparatively small as compared to 5.5% for the Fe/Si system. Among the physical properties studied were magneto-optical Kerr effect[6] (MOKE) and magnetization (magnetic anisotropy) measurements.[7,8] Only rather recently interlayer exchange coupling was discussed in terms of heat-induced effects.[9,10] The first electrical transport measurements on bilayers of Fe and amorphous ZnSe were reported last year.[11] It seems at present that this electric transport study, devoted directly to the original goal of finding systems with a reasonably large magnetoresistance, is only the beginning of a series of similar investigations devoted to ''metal/semiconductor'' heterojunctions, i.e., to layered systems and/or surface structures combining a magnetic metal with a material that is semiconducting as a bulk system. It should be noted that even in the latest experimental studies[9,10] the ZnSe part of the heterojunctions was termed ''amorphous,'' indicating merely that no structural information whatever is available.

Fe/ZnSe heterostructures also raised theoretical interest: Continenza *et al.*[12,13] were the first to actually perform *ab initio* calculations for Fe adlayers on ZnSe(001) (Ref. 12) and for $Fe_n/(ZnSe)_m$ superlattices (Ref. 13). Quite recently, based on the Landauer-Büttiker formalism, MacLaren *et al.*[14,15] have discussed spin-dependent tunneling in epitaxial systems such as Fe/ZnSe/Fe heterostructures for which they found[15] a magnetoresistance ratio (defined there as the difference in conductances for the antiparallel and parallel configuration divided by the conductance in the parallel configuration) that increases with increasing spacer thickness and reaches a value above 0.9 beyond a spacer thickness of about 60 a.u.

In the present study the interlayer exchange coupling, magnetic anisotropy, and perpendicular electric transport are presented for both types of termination, i.e., either Zn or Se, of bcc Fe/ZnSe/Fe heterojunctions. In Sec. II the main theoretical and computational aspects are summarized, whereas Sec. III contains the main results of the present study and is followed by a short discussion and conclusion part. It is important to stress right from the beginning that all ''spin'' and ''spin-orbit'' type effects are included on the same footing in a parameter-free manner because of the uniform fully relativistic spin-polarized approach applied.

## II. THEORETICAL AND COMPUTATIONAL ASPECTS

### A. Self-consistent calculations

The fully relativistic spin-polarized screened Korringa-Kohn-Rostoker method for layered systems[16,17] is applied to calculate the electronic structure and magnetic properties of Fe/ZnSe/Fe heterostructures with growth direction along (100). In particular systems of the type $Fe(100)/Fe_{12}/(ZnSe)_tZn/Fe_{12\pm1}/Fe(100)$ and $Fe(100)/Fe_{12}/(SeZn)_tSe/Fe_{12\pm1}/Fe(100)$, $t$ being the number of repetitions, i.e., heterostructures with Zn and Se termination were investigated. Since according to the setup used for the screened structures constants,[17] the total number $n$ of layers in the intermediate region comprising the left and right Fe buffer to the substrate and the spacer has to be a multiple of three. This particular feature arises from the special shape of

 

the screened structure constants; see, e.g., Ref. 17. Therefore, the number of Fe layers in the right Fe buffer varies from 11 to 13, i.e., $n=24+(2t+1)\pm 1$. In all calculations a bcc-Fe parent lattice[18] is assumed with a lattice spacing $a_0$ of 5.27 a.u. (bulk bcc Fe), i.e., no layer relaxation is considered. In order to determine self-consistently within the local density approximation[19] (LDA) the effective potentials and effective exchange fields for each particular system under consideration a minimum of 45 $\mathbf{k}_\parallel$ points in the irreducible wedge of the surface Brillouin zone (ISBZ) was used. All self-consistent calculations (bulk substrates and semi-infinite system) refer to a ferromagnetic configuration $\mathcal{C}_0$ with the orientation of the magnetization normal to the surface. It should be noted that the use of a Fe bcc parent lattice clearly is an assumption that arises from the need of utilizing two-dimensional lattice Fourier transformations,[17] which in turn are only defined for a common two-dimensional lattice[18] in all layers. Alternatively the parent lattice of the spacer material (zinc blende in the present case) can be assumed, implying, however, that also the lead material has to be of this structure.

### B. Interlayer exchange coupling and magnetic anisotropy energy

The interlayer coupling energy and the anisotropy energy correspond to the (total) energy difference between two given magnetic configurations,

$$\Delta E = E(\mathcal{C}) - E(\mathcal{C}_0), \tag{1}$$

where $\mathcal{C}$ is a magnetic configuration different from $\mathcal{C}_0$. Here this energy difference is evaluated by making use of the magnetic force theorem, which implies that only the reference configuration ($\mathcal{C}_0$) is determined self-consistently within the LDA and $\Delta E$ is replaced by the respective difference in the single-particle part of the grand canonical potential,

$$\Delta E \sim \Delta E_b = \sum_{p=1}^{n} \Delta E_b^p, \tag{2}$$

$$\Delta E_b^p = \int_{\epsilon_b}^{\epsilon_F} [n^p(\epsilon;\mathcal{C}) - n^p(\epsilon;\mathcal{C}_0)](\epsilon - \epsilon_F)\, d\epsilon, \tag{3}$$

which as indicated in Eq. (3) can be written in terms of layer-dependent quantities $\Delta E_b^p$ with $p$ denoting the layer index, $n^p(\epsilon;\mathcal{C})$ the layer-resolved density of states for a given magnetic configuration $\mathcal{C}$, $\epsilon_b$ the (valence) band bottom, and $\epsilon_F$ the Fermi energy of the substrate. In the present paper, all $\Delta E_b$ are evaluated by using a total of 990 $\mathbf{k}_\parallel$ points in the ISBZ, which—as was shown[17] in the case of magnetic anisotropy energies—guarantees well-converged results. It should be noted that according to Eq. (1) $\Delta E_b > 0$ implies that $\mathcal{C}_0$ is the energetically preferred magnetic configuration.

In the case of the interlayer exchange energy two different antiferromagnetic configurations $\mathcal{C}$ were investigated (see also Ref. 20), namely, one in which the orientation of the magnetization was reversed only in the right Fe slab and another one, when in the second (right) half of $n/2$ atomic layers ($n/2-1$ in the case of an odd $n$) the magnetization was switched to antiparallel. As matters of simplicity, the first one will be termed ''asymmetric antiferromagnetic'' configuration and the second one ''symmetric antiferromagnetic'' configuration.

In the case of the magnetic anisotropy energy (MAE), $\mathcal{C}$ refers to a uniform in-plane orientation in all layers. The magnetic anisotropy energy is then, in principle, given as the sum of $\Delta E_b$ in Eq. (2), called the band energy part of the MAE, and the corresponding difference in the magnetic dipole-dipole interaction energy (see also Ref. 17). Here only the band energy part of the MAE is considered, since the physical meaning of the magnetic dipole-dipole interaction for heterojunctions with infinite leads might be misleading for interface properties.

### C. Perpendicular electric transport

For current perpendicular to the planes of the layers (CPP) of a magnetic tunnel junction or multilayered structure, the local electric field varies from layer to layer, so that the measured conductivity is not simply a sum of the two-point conductivities as it is for currents in the plane of the layers. For magnetic tunnel junctions the most prevalent way to calculate the CPP conductivity is to use Landauer's formalism.[14,15] Here we adopt an alternative approach suggested for metallic multilayers, i.e., finding the resistivity tensor by inverting the conductivity;[21,22] we recently applied this method to Fe/Ge/Fe junctions.[25] As we are calculating the electronic structure in a fully relativistic way there is no obvious choice for the electric fields for CPP as there is for nonrelativistic spin-polarized calculations when one posits different electric fields for the spin-up and spin-down states that are found by mandating current conservation in each spin channel. Here we assume there is a common electric field for all the channels of conduction and demand conservation of current after summing over all states; this has been found to be correct for metallic multilayers when there is sufficient spin flip scattering between the up and down spin channels so as to *locally* maintain the voltage or electric field acting on each channel of conduction the same. Thus we are positing that the mixed spin character of our relativistic states is sufficient for us to use a common electric field for all states, while conserving current and still producing a ''giant magnetoresistance'' for perpendicular transport.

The conductivity tensor $\sigma(z,z')$, where $z$ and $z'$ are continuous variables along the surface normal, is mapped onto the conductivity tensor for a layered system,[23,24] $\sigma_{ij}(n)$, $i,j=1,\ldots n$, where $i$ and $j$ denote planes of atoms and $n$ the total number of planes, such that the algebraic structure is conserved:

$$\int \rho(z,z'')\sigma(z'',z') = \delta(z-z'), \quad \sum_k \rho_{ik}(n)\sigma_{kj}(n) = \delta_{ij}. \tag{4}$$

The sheet resistance

$$r(n)=\sum_{i,j=1}^{n}\rho_{ij}(n) \tag{5}$$

then serves as a measure of the mapping.[25] Suppose $\mathcal{C}$ denotes a particular magnetic configuration and $\delta$ is the imaginary part of the complex Fermi energy, $\epsilon_F+i\delta$, that is needed for our calculations; then

$$r(\mathcal{C};n)=\lim_{\delta\to 0}r(\mathcal{C};n;\delta)=\lim_{\delta\to 0}\sum_{i,j=1}^{n}\rho_{ij}(\mathcal{C};n;\delta), \tag{6}$$

where

$$\sum_{k=1}^{n}\rho_{ik}(\mathcal{C};n;\delta)\sigma_{kj}(\mathcal{C};n;\delta)=\delta_{ij}. \tag{7}$$

Furthermore, we define a layer-resolved sheet resistances $r_i(\mathcal{C};n;\delta)$ as

$$r_i(\mathcal{C};n;\delta)=\sum_{j=1}^{n}\rho_{ij}(\mathcal{C};n;\delta), \tag{8}$$

such that according to Eq. (4)

$$r(\mathcal{C};n;\delta)=\sum_{i=1}^{n}r_i(\mathcal{C};n;\delta). \tag{9}$$

It was recently shown[25] that for heterojunctions of the type $\ldots/L_nX_sL_n/\ldots$, where $L_n$ denotes $n$ layers of the electrode material and $X_s$ $s$ layers of spacer, the corresponding sheet resistance $r(\mathcal{C};2n+s;\delta)$ for a given value of $\delta$ and $n\geqslant n_0$ varies linearly with respect to $n$,

$$r(\mathcal{C};2(n+m)+s;\delta)=r(\mathcal{C};2n+s;\delta)+2mk_1(\mathcal{C};\delta),\quad m\in\mathbb{N}^+ \tag{10}$$

$$\lim_{\delta\to 0}k_1(\mathcal{C};\delta)=0, \tag{11}$$

and, furthermore, for a given $n$ and $s$, is linear also in $\delta$, i.e.,

$$r(\mathcal{C};2n+s;\delta)=r(\mathcal{C};2n+s)+\delta k_2(\mathcal{C};2n+s). \tag{12}$$

From these two equations it immediately follows that for $n\geqslant n_0$

$$\lim_{\delta\to 0}r(\mathcal{C};2(n_0+m)+s;\delta)=r(\mathcal{C};2n_0+s),\quad m\in\mathbb{N}^+ \tag{13}$$

i.e., the extrapolation of our calculations for finite $\delta$ permit us to find the resistance provided we have $n\geqslant n_0$. The relevant part for such a heterojunction, $r(\mathcal{C};2n_0+s)$, is therefore defined by the condition that for $n\geqslant n_0$ and for a chosen $\delta>0$ the sheet resistance $r(\mathcal{C};2n+s;\delta)$ starts to change linearly in $n$.

Accordingly, the magnetoresistance is then given as

$$R(2n_0+s)=\frac{r(\mathcal{AP};2n_0+s)-r(\mathcal{P};2n_0+s)}{r(\mathcal{AP};2n_0+s)}, \tag{14}$$

where $\mathcal{AP}$ and $\mathcal{P}$ denote the antiparallel (asymmetric antiferromagnetic configuration—only the orientation of the magnetization in the right Fe buffer and of the substrate is reversed) and parallel magnetic configurations, respectively. As we will show $R(2n_0+s;\delta)\leqslant R(2n_0+s)$; therefore the quantity $R(2n_0+s;\delta)$ can be used for qualitative discussions of the magnetoresistance, keeping in mind that only $R(2n_0+s)$ represents the actual magnetoresistance.

All electric transport calculations were performed by applying the fully relativistic spin-polarized form of the Kubo-Greenwood equation for layered systems[23,24] by using 1830 $\mathbf{k}_\parallel$ points in the ISBZ for the SBZ integrals. In all cases $n_0=11$ was sufficient to obtain linearity for the resistance and we write $s=2t+1$, where $t$ is the number of repetitions of a unit consisting of one Zn and one Se layer. The continuation to the real axis, see Eq. (13) was carried out numerically by means of a linear fit to the values obtained for $\delta=2,\ 2.5$, and 3 mRy.

## III. RESULTS

### A. Electronic structure and magnetic moments

Usually when discussing tunneling in general potential barrier models are applied. In a layered system such models correspond to layer-resolved Madelung potentials. In Fig. 1 these Madelung potentials are displayed for a characteristic case, namely, for a Fe/ZnSe/Fe heterostructure with 12 repetitions. As can be seen from this figure the differences between a Zn- and a Se-terminated structure is basically confined to a few atomic layers near the interfaces. In direction of the leads, i.e., to the left and to the right of the interfaces, the Madelung potentials rapidly approach zero (bulk value); in the interior of the spacer the Zn-like layers have negative and the Se-like layers weakly positive Madelung potentials; the latter act therefore as a repeated set of potential barriers. The Madelung potentials shown in Fig. 1 can be considered as potential barriers in a very qualitative one-dimensional model of electron probabilities viewed when resolved by layers.

Substantial differences between the two types of terminations can be seen also in corresponding (layer-resolved) magnetic moments. In Fig. 2 again a Fe/ZnSe/Fe heterostructure with 12 repetitions serves as characteristic example. In Zn-terminated heterostructures essentially only the magnetic moment in the Fe layer forming the interface is reduced with respect to the value in the leads, whereas in Se-terminated heterostructures the last two Fe layers show strong variations: in the last but one Fe layer before the interface the magnetic moment is substantially enhanced and differs by almost $1\mu_B$ from the magnetic moment in the Fe layer forming the interface. Similar effects can be read off from the tiny induced moments in the spacer layers. Figure 2, but also Fig. 1, suggests that in order to describe the electronic structure and magnetic properties of Fe/ZnSe interfaces at least three layers on each side of the interface ought to be taken into account.

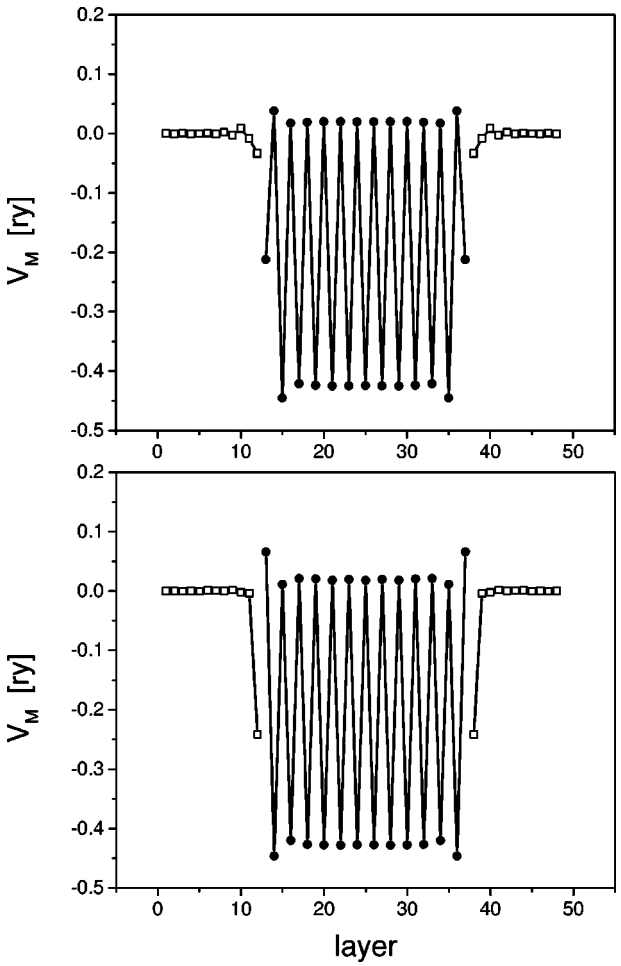


FIG. 1. Layer-resolved Madelung potentials in $Fe(100)/(ZnSe)_{12}/Fe(100)$. Top: Zn termination. Bottom: Se termination. Open squares: Fe. Circles: spacer.

### B. Interlayer exchange energy and magnetic anisotropy energy

The two entries in Fig. 3, showing the interlayer exchange coupling in Fe/ZnSe/Fe heterostructures, refer to the two different antiferromagnetic configurations considered, namely the asymmetric (top) and the symmetric one (bottom). The shape of the curves in both entries is identical, the only difference being the so-called bias, i.e., the asymptotic value of the interlayer exchange coupling as the spacer thickness becomes very large. As can be seen from Fig. 3, Zn-terminated heterostructures are antiferromagnetically coupled up to a spacer thickness of about 15 Å and then start to oscillate weakly between the ferro- and the antiferromagnetic configuration. The behavior of Se-terminated heterostructures is completely different: for thin spacers there are distinct regions of ferro- and antiferromagnetic coupling, only beyond about 20 Å weak oscillations set in. The small bias that distinguishes the asymmetric from the symmetric case can be important for certain applications since the size of this bias reflects the number of (additional) spacer layers in which the orientation of the magnetization is reversed (see also the discussion in Ref. 20).

In Fig. 4 the band energy part $\Delta E_b$ of the magnetic anisotropy energy is displayed as a function of the spacer thickness for both types of termination. It is obvious that different terminations cause different characteristic behavior: for Zn-terminated heterostructures the orientation of the magnetization is mostly in-plane, while for Se-terminated heterostructures the band energy part of the anisotropy energy favors a perpendicular orientation. In Fig. 5, for a typical example, namely for 12 repetitions of ZnSe, a layerwise decomposition of $\Delta E_b$ is plotted. From this figure one easily can see that the spacer part of the heterojunctions adds very little to $\Delta E_b$: it is essentially the first 3–4 Fe layers next to the interface that account for the actual value of $\Delta E_b$. It is interesting to note that in Zn-terminated heterostructures the contribution from the Fe layer forming the interface has a negative value, whereas from the same layer in the Se-terminated heterostructure the contribution is reasonably large and positive: it is essentially this layer that generates the differences to be seen in Fig. 4. However, as compared to (magnetic) metal overlayers on a metallic substrate,[17] $\Delta E_b$ is rather small, namely, less than 0.5 meV; the orientation of the magnetization (perpendicular versus in-plane) in the vicinity of the interfaces does not seem to be a decisive property of Fe/ZnSe/Fe heterostructures.

### C. Perpendicular electric transport

Figure 6 illustrates the numerical procedures applied to evaluate the magnetoresistances. In the top part of this figure the sheet resistance for the parallel and antiparallel configurations for a Se-terminated Fe/ZnSe/Fe heterostructure with 12 repetitions of the building unit ZnSe is plotted versus the number $n$ of Fe (buffer) layers. As can be seen for a finite imaginary part $\delta$ of the Fermi energy these two sheet resistances indeed grow linearly with the number of Fe buffer layers, provided $n_0$ is large enough [see Eq. (13)]. Obviously, the present choice of $n_0=11$ is well within the linear regime described by Eq. (10). In fact any $n_0 \geqslant 4$ would serve the same purpose. In the lower half of Fig. 6, for the same system the numerical continuation of the calculated sheet resistances $r(\mathcal{C};2n_0+s;\delta)$ to the real energy axis is shown in terms of a linear fit; from this procedure an error for the magnetoresistance of about 2% has to be expected. It should be noted, that for $\delta<2.0$ mRy the surface Brillouin zone integrations that have to be carried out become very difficult to converge with respect to the number of **k** points; for this reason we have not carried out such calculations. As can be seen from the insets in Fig. 6, the main error arises from the sheet resistance in the antiparallel configuration; we believe this comes from the additional numerical errors incurred when rotating the magnetization into the antiparallel configuration.[17]

It turned out that in all cases investigated the constant $k_2(\mathcal{C};n)$ in Eq. (12) has the following properties:

$$k_2(\mathcal{C};n)\begin{cases} >0; & \text{parallel configuration} \\ <0; & \text{antiparallel configuration} \end{cases} \tag{15}$$

i.e., in the parallel configuration the sheet resistance increases with increasing imaginary part $\delta$ of the Fermi energy, whereas in the antiparallel configuration the opposite applies.

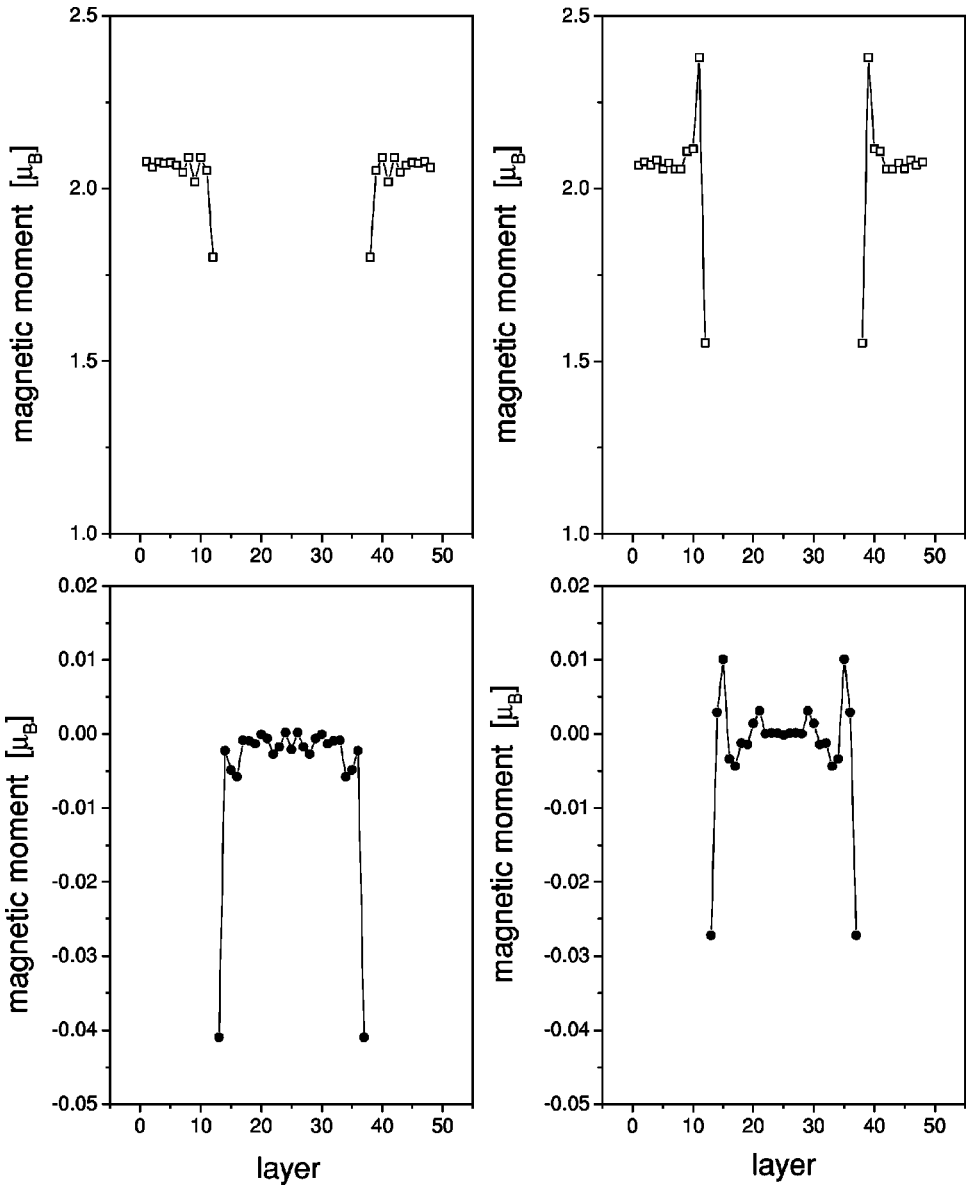


FIG. 2. Magnetic moments in Fe(100)/$(ZnSe)_{12}$/Fe(100). Left: Zn termination. Right: Se termination. Top: Fe-moments. Bottom: magnetic moments in the spacer.

This behavior, which causes the magnetoresistance to increase with decreasing $\delta$, can be understood as follows: in the parallel configuration the lower resistance is indicative of ''metallic conduction'' of a (poor) metal while in the antiferromagnetic configuration a ''tunneling'' type of conduction seems to be present.[26] This particular feature can also be seen in Fig. 7 in which the sheet resistances in Se-terminated Fe/(ZnSe)/Fe heterostructures are displayed with respect to the spacer thickness. In this figure, which contains resistances calculated for two very thick spacers, the sheet resistance for the antiparallel alignment is considerably bigger than the one for the parallel alignment. Aside from the gyrations at very small thicknesses the curves for $\delta=2$ mRy and for a vanishing imaginary part are very similar in shape.

In Fig. 8 we plot the product of the sheet resistances (as continued to the real energy axis) and the number of repetitions $t$ versus the number of repetitions for both types of termination. These are fitted to

$$r(\mathcal{P};2(n_0+t)+1)t \equiv r(\mathcal{P};t)t = C_{\mathcal{P}} + k_{\mathcal{P}} t \qquad (16)$$

and

$$r(\mathcal{AP};2(n_0+t)+1)t \equiv r(\mathcal{AP};t)t = C_{\mathcal{AP}} + k_{\mathcal{AP}} t. \qquad (17)$$

As can be seen from the figures these products are linear in $t$, i.e., the spacer thickness times sheet resistance grows linear with the spacer thickness, and in Table I we list the parameters obtained by fitting the plots in Fig. 8. Clearly enough such a fit can also be made either in terms of the total number of spacer layers, $s=2t+1$, or with respect to $d=2(2t+1)/a_0$, where $a_0$ is the lattice parameter of the underlying parent lattice. It should be noted that for both types of termination the slopes of the sheet resistances for the parallel and antiparallel magnetic configurations are different. By using Eqs. (16) and (17) the difference in the sheet resistance between the antiparallel and the parallel alignments can be formulated as

$$\Delta r(t) \equiv r(\mathcal{AP};t) - r(\mathcal{P};t) = \frac{C_{\mathcal{AP}} - C_{\mathcal{P}}}{t} + k_{\mathcal{AP}} - k_{\mathcal{P}}, \qquad (18)$$

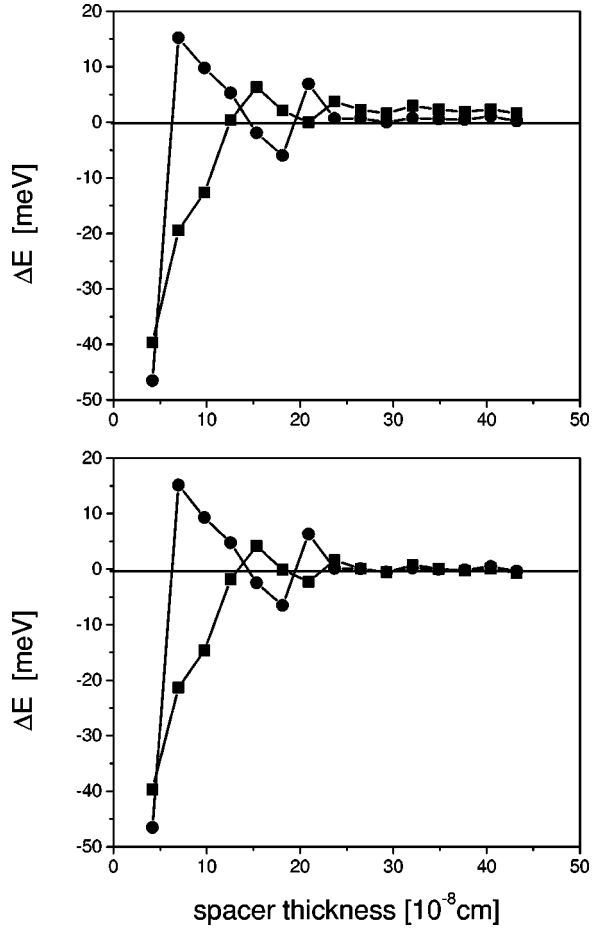


FIG. 3. Interlayer exchange coupling in Fe(00)/ZnSe/Fe(100) heterostructures as a function of the spacer thickness. Top: ''asymmetric'' antiferromagnetic configuration. Bottom: ''symmetric'' antiferromagnetic configuration. Squares: Zn termination. Circles: Se termination.

which in turn implies that

$$\lim_{t\to\infty}[\Delta r(t)] = k_{\mathcal{AP}} - k_{\mathcal{P}}, \tag{19}$$

i.e., with increasing spacer thickness $\Delta r(t)$ becomes a constant. This is very important since it means that even for Fe/ZnSe/Fe heterojunctions with a very thick spacer part the sheet resistances (and consequently the corresponding resistances) are distinctly different in the parallel and the antiparallel alignment, i.e., we find substantial magnetoresistance. This is confirmation that our postulate of a common electric field is able to produce an MR in these structures with our fully relativistic code.

In Fig. 9 the magnetoresistance $R(t)$ with respect to the spacer thickness, see Eq. (14), is displayed for both types of termination. Also shown in this figure is the magnetoresistance obtained by using Eqs. (16) and (17), which, as can be seen, describes rather well the shapes of the curves corresponding to the calculated values (continued to the real energy axis). It is important to note that since $\Delta r(t)$ *and* $r(\mathcal{AP};t)$ remain finite as $t$ becomes very large, the corresponding magnetoresistance also becomes a constant:

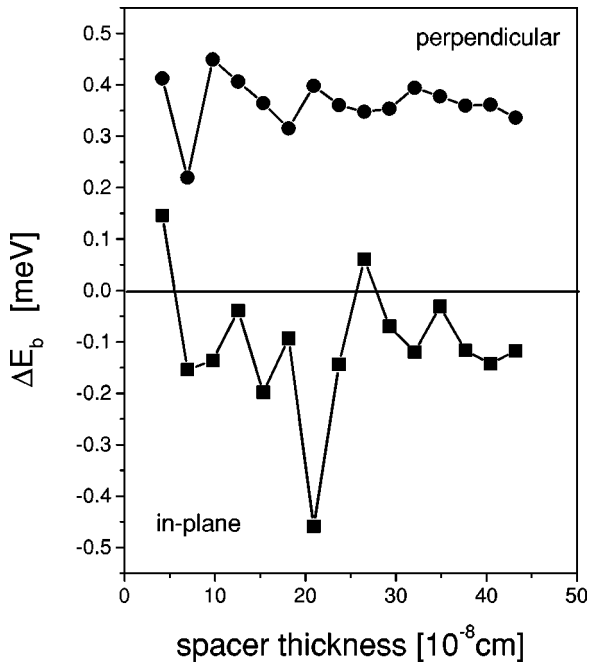


FIG. 4. Band energy part of the magnetic anisotropy energy in Fe(100)/ZnSe/Fe(100) heterostructures as a function of the spacer thickness. Squares: Zn termination. Circles: Se termination.

$$\lim_{t\to\infty} R(t) = 1 - \frac{k_{\mathcal{P}}}{k_{\mathcal{AP}}}. \tag{20}$$

While the $R(t)$ of magnetic tunnel junctions are relatively insensitive to the thickness of the barriers, the resistance of our ZnSe spacer is probably not that high to qualify it as a barrier with a resistance typical of insulators. Finally in Fig. 10 an attempt is made to comment on the different behavior of Zn- and Se-terminated heterostructures by partitioning $\Delta r(t)$ [see Eq. (9)] into contributions arising from different parts of the heterostructure, namely, the left and right electrodes (leads) $L_{\text{left}}$ and $L_{\text{right}}$, the interface regions between electrodes and spacer, $I_{\text{left}}$ and $I_{\text{right}}$, and the remaining spacer part $S$,

$$\Delta r(t;\delta) = \Delta r_{L_{\text{left}}}(t;\delta) + \Delta r_{L_{\text{right}}}(t;\delta) + \Delta r_{I_{\text{left}}}(t;\delta) + \Delta r_{I_{\text{right}}}(t;\delta) + \Delta r_{S}(t;\delta). \tag{21}$$

As an example heterostructures with 21 repetitions of ZnSe are considered and the interface region is chosen to consist of the actual interface plus three atomic layers to the left and right of it, i.e., for the Zn-terminated heterostructure the interface region is of the form $Fe_3$/FeZn/SeZnSe. As can be seen from this figure for the Se-terminated structure the magnetoresistance $\Delta r(s;\delta)$ ($\delta = 2$ mRy) is entirely determined by the contributions from the two interface regions, while in the Zn-terminated structure the spacer part reduces these contributions. The difference between the two kinds of termination is not surprising recalling Fig. 2: in the spacer region of the Zn-terminated system the magnetic moments show more rapid variations than in the spacer region of the

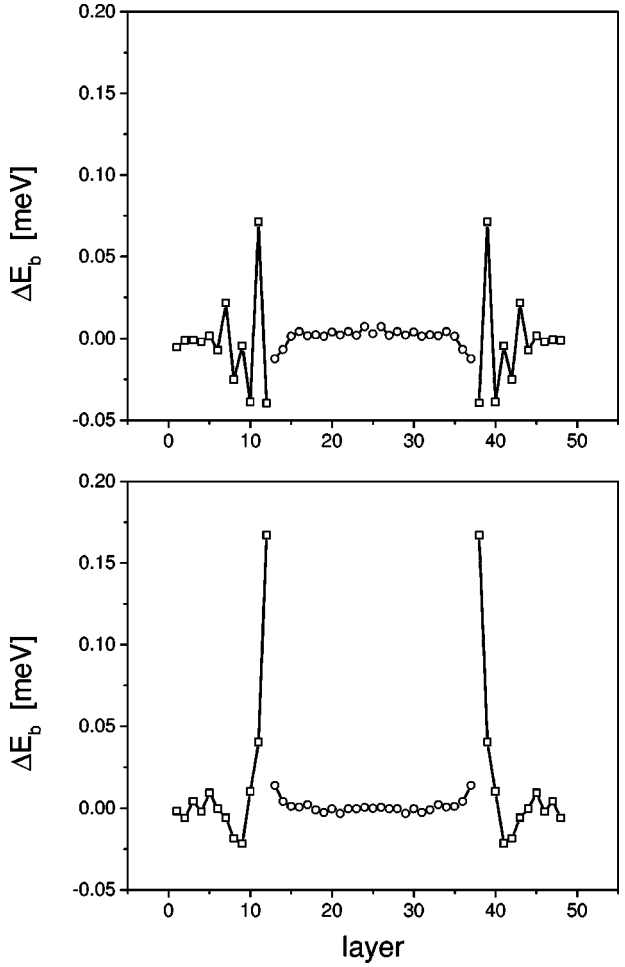


FIG. 5. Layer-resolved band energy part of the anisotropy energy in Fe(100)/$(ZnSe)_{12}$/Fe(100). Top: Zn-termination. Bottom: Se-termination. Squares: Fe layers. Circles: spacer layers.

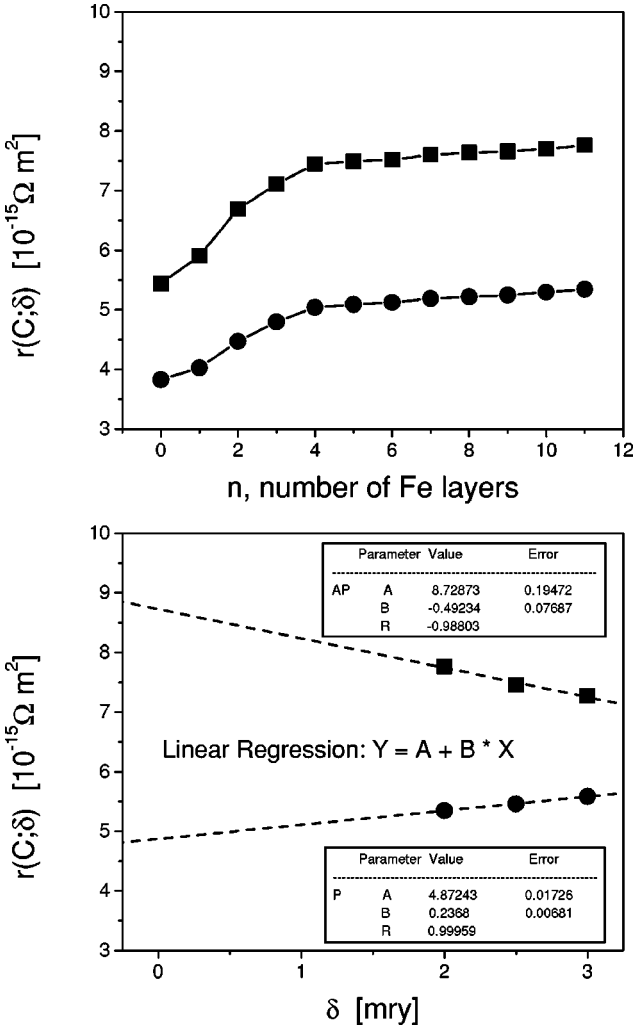


FIG. 6. Sheet resistances $r(C;\delta)$ in Se-terminated Fe(100)/$(ZnSe)_{12}$/Fe(100) heterostructures as a function of the number of Fe buffer layers (top, $\delta = 2$ mRy) and as a function of the imaginary part $\delta$ of the complex Fermi energy (bottom). The inset shows the parameters for the linear fits (dashed lines). Circles and squares refer to the ferro- (parallel) and antiferromagnetic (antiparallel) configuration, respectively.

Se-terminated system. In both cases it is clear that the interface regions contribute most of the difference in the sheet resistances.

## IV. DISCUSSION AND CONCLUSION

Walser *et al.*[9,10] discuss the spin polarization of secondary electrons at remanence of the top Fe layer (15 Å) of an Fe/amorphous-ZnSe (wedge)/Fe sample versus the ZnSe spacer thickness. Although their samples are grown on 70 Å Co on top of a Cu(100) substrate and the lower Fe layer is rather thin (5 Å), interesting comparisons can be made to the present results concerning the interlayer exchange coupling. They find that in a spacer thickness range between 18 and 22 Å the polarization signal is negative, which in turn implies the occurrence of antiferromagnetic coupling. Between 23 and 25 Å and for low temperatures this polarization is again positive (ferromagnetic coupling). Above this thickness the coupling seems to remain ferromagnetic. Furthermore, for thicker spacers an interesting temperature behavior was discovered by which a switching from ferromagnetic to antiferromagnetic coupling can be achieved.

Comparing now these findings with Fig. 3, one can see that the theoretically calculated interlayer exchange coupling for the Se-terminated heterostructures switches at about 15 Å from ferromagnetic to antiferromagnetic and is again ferromagnetic above 20 Å . The fact that in the above-mentioned experiments the coupling seems to remain ferromagnetic above about 25 Å seems to indicate that a very small bias is seen (see also Fig. 3, top). The calculated regime of antiferromagnetic coupling in the case of Se-terminated heterostructures agrees therefore quite well with the experimental findings. Furthermore, since Zn-terminated heterostructures behave totally different—they are ferromagnetically coupled for spacer thicknesses between about 12 and 20 Å —it is tempting to argue that in the experimental study predominantly a Se-terminated spacer was present.

Very recently also an electric transport study was published[11] by the same group of researchers. Although in this study the main concern was devoted to the temperature

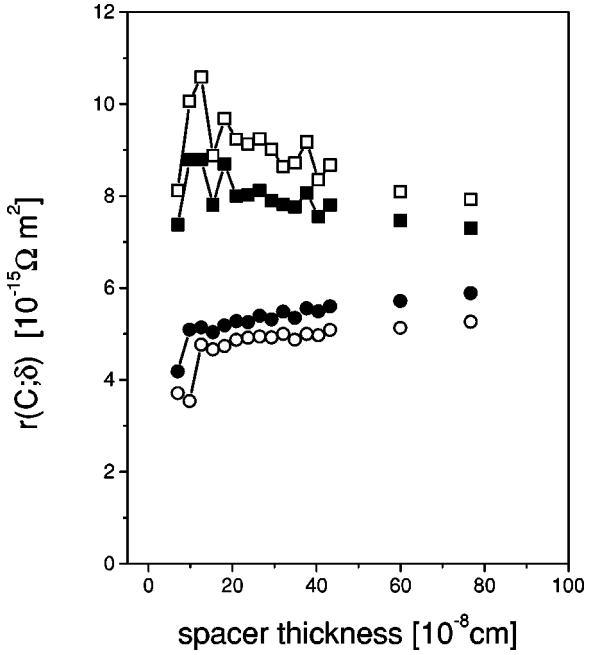


FIG. 7. Sheet resistance $r(\mathcal{C};\delta)$ in Fe(100)/ZnSe/Fe(100) heterostructures with Se termination as a function of the spacer thickness. Circles: ferromagnetic (parallel) configuration. Squares: antiferromagnetic (antiparallel) configuration. Full symbols refer to an imaginary part of the complex Fermi energy of 2 mRy; open symbol to the values continued to the real energy axis.

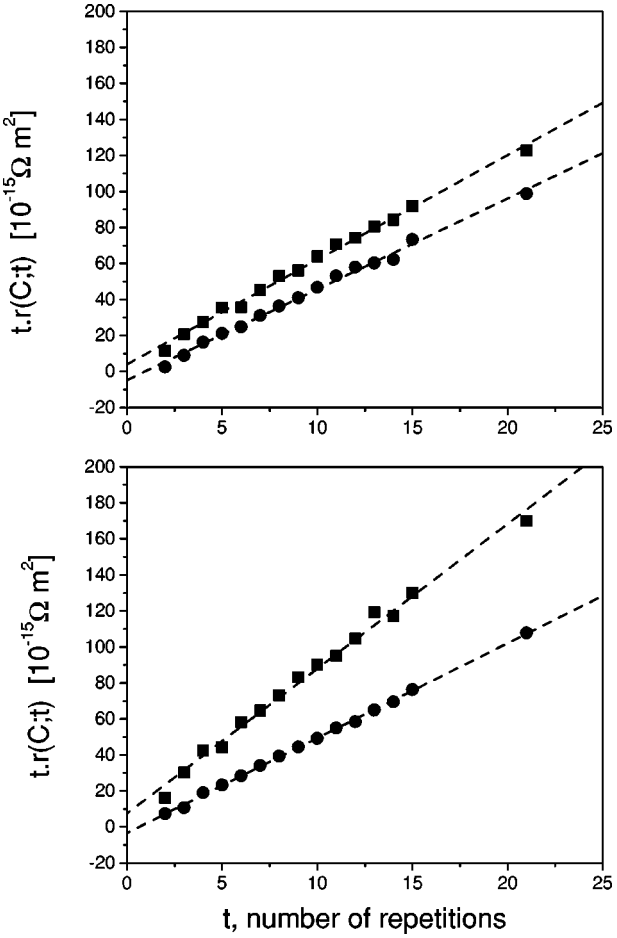


FIG. 8. Product of sheet resistances (continued to the real energy axis) $r(\mathcal{C};t)$ and the number of repetition $t$ versus $t$. Top: Zn termination. Bottom: Se termination. Circles and squares refer to the parallel and antiparallel configuration, respectively.

dependence of the conductivity, a few general conclusions made appear to support the present results. First of all ''*as a general observation*'' they report ''*that the conductivities do not depend greatly on the thickness of the ZnSe layers.*'' When putting an 18 Å thick layer of Fe on top of 150 Å of ZnSe they observe a ''*metallic contribution*'' to the conductivity, whose temperature dependence is still ''*semiconductor-like to some extent.*'' Furthermore, they speculate that defect states at the interfaces between the metal and the semiconductor are of crucial importance for both the electric transport properties and the interlayer exchange coupling.

From Figs. 7 and 8 as well as from Eqs. (18) and (19) it is evident that the conductivity (for a particular magnetic configuration) indeed does not depend much on the thickness of the spacer. Furthermore, as we show in Fig. 10 that the magnetoresistance in Fe/ZnSe/Fe heterostructures is mostly due to contributions from the interfaces, it is not surprising that any kind of interdiffusion or other types of roughness at the interfaces strongly modulates the electric transport properties. The simultaneous occurrence of a metallic and a semiconductor mode of conduction recorded in experiment appears to be very much related to the different slopes of the sheet resistances with respect to the imaginary part of the complex Fermi energy discussed in the context of Fig. 6. As already mentioned in the Introduction MacLaren *et al.*[14,15] find for Fe/ZnSe/Fe heterostructures ''a tunneling conductance at large thicknesses that is dominated by majority electrons,'' which in turn differs from what they observed from calculations in which the barrier was a constant potential.[27] Since their calculations were performed without spin-orbit coupling, it is difficult to compare them with the present fully relativistic spin-polarized results, which of course include the spin orbit to all orders of the usual perturbative expansion, since the two ''spin channels'' are coupled to each other. It should be noted that in the case of the leads these authors use a parent lattice with two inequivalent Fe atoms, and a Zn (Se) atom and an empty sphere per two-dimensional unit cell for the spacer material, i.e., they mim-

TABLE I. Fitting parameters for sheet resistances $r(C;t)$ in the the range $2 \leqslant t \leqslant 21$.

| | Zn termination | Se termination |
|---|---|---|
| $C_{\mathcal{P}}$ | -4.7671 | -3.3176 |
| $C_{\mathcal{AP}}$ | 3.9518 | 7.4732 |
| $k_{\mathcal{P}}$ | 5.0443 | 5.2694 |
| $k_{\mathcal{AP}}$ | 5.8156 | 8.0441 |
| $R_{\mathcal{P}}$ | 0.9975 | 0.9958 |
| $R_{\mathcal{AP}}$ | 0.9974 | 0.9995 |

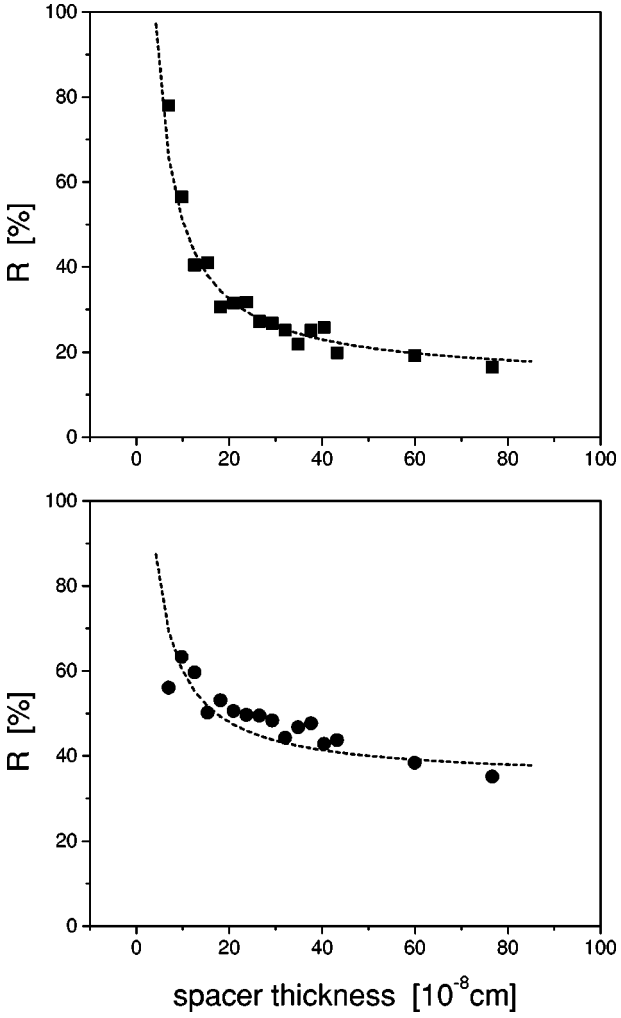


FIG. 9. Magnetoresistance $R(t)$ in Fe(100)/ZnSe/Fe(100) heterostructures as a function of the spacer thickness. Top: Zn termination. Bottom: Se termination. The squares refer to the continued $\delta=0$ values; the dashed lines to the magnetoresistance using the fitted sheet resistances.

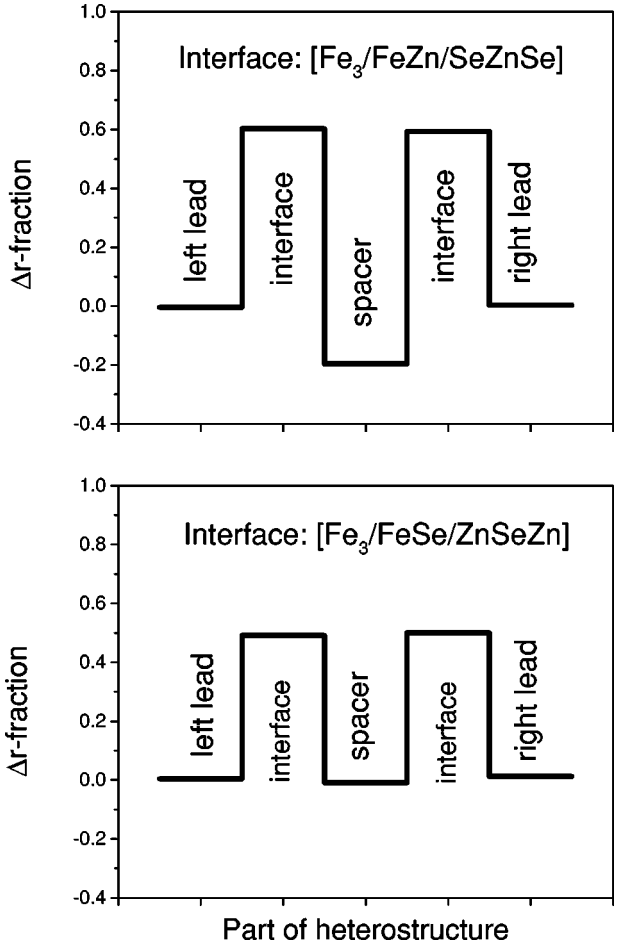


FIG. 10. Normalized fractions of the difference in the sheet resistance between the antiferromagnetic and the ferromagnetic configuration in $Fe(100)/(ZnSe)_{21}/Fe(100)$ [see Eq. (21)]. The various regions of the heterostructure are given explicitly.

ick a zinc blende structure (parent lattice) for the whole system. Also for this reason a comparison to their results is not quite appropriate.

In conclusion, it can be said that (1) Se-terminated Fe/ZnSe/Fe heterojunctions show a regime of spacer thicknesses in which—in agreement with experimental data—antiferromagnetic coupling occurs; (2) magnetic anisotropy effects at the interfaces seem to be of little importance; and (3) the difference in the sheet resistances for the antiparallel and parallel configurations, as well as the magnetoresistance, remain finite as the spacer thickness becomes very large. For Zn-terminated structures this ''asymptotic'' magnetoresistance is about 13%, for Se-terminated structures about 34%. By using the other kind of definition for the magnetoresistance, namely that with respect to the sheet resistance in the parallel configuration, $\Delta\mathbf{r}(t)/\mathbf{r}(\mathcal{P};t)$, the corresponding ratios are 15 and 52%. Finally, a point has to be stressed again: as long as one does experiments in which the spacer is ''amorphous,'' parent lattices[18] with respect to the (bulk) lattice of the spacer do not make any physical or (group) theoretical sense.

## ACKNOWLEDGMENTS

We thank Professor P. M. Levy for a careful reading of this manuscript. This paper resulted from a collaboration partially funded by the RTN network ''Magnetoelectronics'' (Contract No. RTN1-1999-00145). Financial support was provided also by the Center for Computational Materials Science (Contract No. GZ 45.451), and the Austrian Science Foundation (Contract No. P12146), the Hungarian National Science Foundation (Contract No. OTKA T030240 and T029813). We also wish to thank the computing center IDRIS at Orsay where a part of the calculations was performed on a Cray T3E machine.

[1] B. T. Jonker and G. A. Prinz, J. Appl. Phys. **69**, 2938 (1991).
[2] K. Bierleutgeb, H. Sitter, H. Krenn, and H. Seyringer, Phys. Status Solidi B **220**, 41 (2000).
[3] E. Reiger, E. Reinwald, G. Garreau, M. Ernst, M. Zölfl, S. Bauer, H. Preis, and G. Bayreuther, J. Appl. Phys. **87**, 5923 (2000).
[4] H. Abad, B. T. Jonker, C. M. Cotell, and J. Krebs, J. Vac. Sci. Technol. B **13**, 716 (1995).
[5] R. Dahmani, L. Salamanca-Riba, N. V. Nguyen, D. Chandler-Horowitz, and B. T. Jonker, J. Appl. Phys. **76**, 514 (1994).
[6] H. Wang, H. R. Zhai, H. Y. Zhang, M. Lu, B. X. Gu, L. Zhang, Y. H. Liu, X. D. Ma, and L. M. Mei, J. Magn. Magn. Mater. **104**, 1827 (1992).
[7] J. J. Krebs, B. T. Jonker, and G. A. Prinz, J. Appl. Phys. **61**, 3744 (1987).
[8] S. A. Oliver, C. Vittoria, J. J. Krebs, B. T. Jonker, and G. A. Prinz, J. Appl. Phys. **65**, 2799 (1989).
[9] P. Walser, M. Hunziker, and M. Landolt, J. Magn. Magn. Mater. **200**, 95 (1999).
[10] P. Walser, M. Hunziker, T. Speck, and M. Landolt, Phys. Rev. B **60**, 4082 (1999).
[11] M. Hunziker and M. Landolt, Surf. Sci. **468**, 187 (2000).
[12] A. Continenza, S. Massidda, and A. J. Freeman, J. Magn. Magn. Mater. **78**, 195 (1989).
[13] A. Continenza, S. Massidda, and A. J. Freeman, Phys. Rev. B **42**, 2904 (1990).
[14] J. M. MacLaren, W. H. Butler, and X.-G. Zhang, J. Appl. Phys. **83**, 6521 (1998).
[15] J. M. MacLaren, X.-G. Zhang, W. H. Butler, and Xindong Wang, Phys. Rev. B **59**, 5470 (1999).
[16] L. Szunyogh, B. Újfalussy, and P. Weinberger, Phys. Rev. B **51**, 9552 (1995).
[17] P. Weinberger and L. Szunyogh, Comput. Mater. Sci. **17**, 414 (2000).
[18] For a discussion of the concept of parent lattices see, e.g., P. Weinberger, Philos. Mag. B **75**, 509 (1997).
[19] S. H. Vosko, L. Wilk, and M. Nusair, Can. J. Phys. **58**, 1200 (1980).
[20] A. Vernes, P. Weinberger, C. Blaas, P. Mohn, L. Szunyogh, P. M. Levy, and C. Sommers, Philos. Mag. B (to be published).
[21] P. M. Levy, in *Solid State Physics*, edited by H. Ehrenreich and D. Turnbull (Academic Press, Cambridge, MA, 1994), Vol. 47, pp. 367–462.
[22] P. M. Levy and I. Mertig, in *Spin-Dependent Transport in Magnetic Nanostructures*, edited by T. Shinjo and S. Maekawa (Gordon and Breach, New York, in press).
[23] P. Weinberger, P. M. Levy, J. Banhart, L. Szunyogh, and B. Újfalussy, J. Phys.: Condens. Matter **8**, 7677 (1996).
[24] C. Blaas, P. Weinberger, L. Szunyogh, P. M. Levy, and C. Sommers, Phys. Rev. B **60**, 492 (1999); C. Blaas, P. Weinberger, L. Szunyogh, C. Sommers, and P. M. Levy, Phys. Rev. B **63**, 224408 (2001).
[25] P. Weinberger, L. Szunyogh, C. Blaas, and C. Sommers (unpublished).
[26] S. Zhang and P. M. Levy, Phys. Rev. B **57**, 5336 (1998).
[27] J. M. MacLaren, X.-G. Zhang, and W. H. Butler, Phys. Rev. B **56**, 11 827 (1997).